

# The Enrichment History of Baryons in the Universe

Romeel Davé & Benjamin D. Oppenheimer

*Astronomy Department, University of Arizona, Tucson, AZ 85721*

19 June 2018

## ABSTRACT

We present predictions for the cosmic metal budget in various phases of baryons from redshift  $z = 6 \rightarrow 0$ , taken from a cosmological hydrodynamic simulation that includes a well-constrained model for enriched galactic outflows. We find that substantial amounts of metals are found in every baryonic phase at all epochs, with diffuse intergalactic gas dominating the metal budget at early epochs and stars and halo gas dominating at recent epochs. We provide a full accounting of metals in the context of the missing metals problem at  $z \approx 2.5$ , showing that  $\sim 40\%$  of the metals are in galaxies, and the remainder is divided between diffuse IGM gas and shocked gas in halos and filamentary structures. Comparisons with available observations of metallicity and metal mass fraction evolution show broad agreement. We predict stars have a mean metallicity of one-tenth solar already at  $z = 6$ , which increases slowly to one-half solar today, while stars just forming today have typically solar metallicity. Our HI column density-weighted mean metallicity (comparable to Damped Ly $\alpha$  system metallicities) slowly increases from one-tenth to one-third solar from  $z = 6 \rightarrow 1$ , then falls to one-quarter solar at  $z = 0$ . The global mean metallicity of the universe tracks  $\sim 50\%$  higher than that of the diffuse phase down to  $z \sim 1$ , and by  $z = 0$  it has a value around one-tenth solar. Metals move towards higher densities and temperatures with time, peaking around the mean cosmic density at  $z = 2$  and an overdensity of 100 at  $z = 0$ . We study how carbon and oxygen ions trace the path of metals in phase space, and show that O III–O VII lines provide the most practical option for constraining intergalactic medium metals at  $z \lesssim 2$ .

**Key words:** intergalactic medium, galaxies: abundances, galaxies: evolution, cosmology: theory, quasars: absorption lines, methods: N-body simulations

## 1 INTRODUCTION

Heavy elements are produced exclusively in stars, and then distributed throughout the Universe through supernovae and stellar winds. As such, they provide a unique tracer of the star formation and feedback processes that are central to understanding how galaxies form and evolve. Metals are present at the earliest observable epochs: The farthest known quasar at  $z = 6.4$  shows substantial enrichment despite being less than 1 Gyr old (Barth et al. 2003), and metals are seen in the intergalactic medium (IGM) at  $z \gtrsim 6$  (Becker et al. 2006; Ryan-Weber, Pettini, & Madau 2006; Simcoe 2006). At lower redshifts, the galaxy mass-metallicity relation has been quantified out to  $\sim 2$  (Tremonti et al. 2004; Savaglio et al. 2005; Erb et al. 2006), intracluster gas metallicities have been constrained out to  $z \sim 1$  (Rosati et al. 2004) and the IGM is observed in metal lines nearly continuously from  $z \sim 6 \rightarrow 0$ .

Pettini (1999) first noted the interesting fact that the metals seen in Lyman break galaxies at  $z \sim 2 - 3$  fall well

short of the amount expected to be produced by the stars in those galaxies. This is known as the *missing metals problem*. It implies that most metals must either reside outside of galaxies, or be in some non-observable form in or around galaxies. Attempts to quantify metals in the IGM (Ferrara, Scannapieco & Bergeron 2005, hereafter FSB05) or other galaxy populations such as sub-millimeter galaxies (Bouché, Lehnert & Péroux 2006a) or damped Lyman alpha (DLA) systems (Prochaska et al. 2006) have not clearly been able to account for the shortfall, though uncertainties remain substantial (Bouché, Lehnert & Péroux 2006b, hereafter BLP06). Virtually every galaxy class and environment examined seems to contain a small but non-trivial amount of metals, so it appears that metal pollution has been curiously democratic. As the distribution of metals in various environments and at various epochs becomes better measured, this provides important constraints into galactic feedback processes.

A theoretical framework for understanding these wide ranging observations is provided by simulations of galaxy formation that include metal production and distribu-

arXiv:astro-ph/0608268v2 11 Oct 2006

tion mechanisms. The pioneering work of Cen & Ostriker (1999b) using cosmological hydrodynamic simulations highlighted some basic trends arising in such models, such as the early enrichment of galaxies and the natural establishment of a metallicity gradient with cosmic overdensity. Using more advanced, higher-resolution cosmological simulations, Thacker, Scannapieco, & Davis (2002) studied global metal enrichment from dwarf galaxies down to  $z = 4$ , and showed that it is possible to enrich the IGM at early times to a value broadly consistent with data while producing dwarf galaxies with enrichment levels similar to local dwarfs.

An alternative approach was taken by Calura & Matteucci (2004), who used detailed chemical evolution models for various galaxy types together with observations of luminosity functions in those types to construct the evolution of metals in galaxies, intracluster gas, and IGM gas. While their models make detailed predictions for individual elements in various galaxy classes, they do not embed the predictions within an *ab initio* hierarchical structure formation framework, relying instead on passively evolving observed luminosity functions back in time. Still, this provides some interesting predictions that are not dissimilar to those presented here. In Calura & Matteucci (2006) they extend their approach to study IGM enrichment, and suggest that winds with velocities exceeding 1000 km/s are required to pollute the IGM to observed levels.

In Oppenheimer & Davé (2006, hereafter OD06) we took such studies to the next level of sophistication, using cosmological simulations that incorporate enriched kinetic feedback in a full hierarchical structure formation setting. Our models, employing outflow scaling relations taken from local starburst data, showed remarkable success at reproducing observations of C IV enrichment in the IGM from  $z \sim 6 \rightarrow 2$ . Matching these data generally required highly mass loaded but low velocity winds from early galaxies, so as to eject a substantial metal mass into the IGM without overheating it. Such scalings naturally arise in momentum-driven wind scenarios (Murray, Quatert, & Thompson 2005) that are also favored by local outflow observations (Martin 2005; Rupke, Veilleux & Sanders 2005), providing an intriguing connection between outflows at all epochs. In Davé, Finlator & Oppenheimer (2006) we show that significant early feedback is also necessary in order to suppress reionization-epoch star formation. In Finlator, Davé & Oppenheimer (in preparation) we show that the resulting galaxy mass-metallicity relation from our favored outflow models agrees well with observations at  $z \sim 2$ . These successes suggest that we now have a plausible structure formation framework with which to study the global evolution of metals in the Universe.

In this paper we use cosmological hydrodynamic simulations incorporating our most successful feedback model from OD06 (described in §2.1) to study the evolution of metals in various baryonic phases in the Universe from  $z = 6 \rightarrow 0$  (§2.2) and provide quantitative answers for the missing metals problem (§2.3). We go on to compare the metallicities in those phases with observations (§2.4), showing broad agreement. We make predictions for how metals evolve in cosmic phase space (§3.1), and study how different oxygen and carbon ions may be used to probe various regimes of phase space (§3.2). We present our conclusions in §4.

## 2 METAL EVOLUTION

### 2.1 Simulations

We run a cosmological hydrodynamic simulation using GADGET-2 (Springel & Hernquist 2002, 2003a) with improvements as described in OD06. Our run has  $2 \times 256^3$  particles in a randomly-generated volume of  $(32h^{-1}\text{Mpc})^3$ , with an equivalent Plummer softening length of  $2.5h^{-1}\text{kpc}$  (comoving). Initial conditions were generated using an Eisenstein & Hu (1999) power spectrum, assuming a concordance cosmology (Spergel et al. 2003) having  $\Omega = 0.3$ ,  $\Lambda = 0.7$ ,  $n = 1$ ,  $H_0 = 70 \text{ km s}^{-1} \text{ Mpc}^{-1}$ , and  $\sigma_8 = 0.9$ . The simulation was started at  $z = 159$ , in the linear regime, and evolved to  $z = 0$ . We include metal-line cooling by augmenting the primordial cooling rate calculated as described in Katz et al. (1996) with the difference in cooling rates between the primordial and metal-enriched collisional ionization equilibrium models of Sutherland & Dopita (1993). Star formation is modeled in a multi-phase manner as described in Springel & Hernquist (2003a), occurring in regions sufficiently dense to undergo multi-phase collapse, with the threshold density depending on the metallicity through the cooling rate.

We employ a momentum-driven wind model as described in OD06, in particular the *vzw* model, which provides the overall best match to the C IV observations considered. In our heuristic outflow model, a star forming particle has a probability to enter a wind that is proportional to the assumed mass loading factor, and if selected it is given a velocity kick. In the *vzw* prescription, the wind velocity is proportional to the galaxy velocity dispersion, which we estimate from the local value of the gravitational potential. The value of the velocity kick has some spread associated with an observed spread in the the luminosity factor (Rupke, Veilleux & Sanders 2005); see Oppenheimer & Davé (2006) for full formula. As predicted in a momentum-driven wind model (e.g. Murray, Quatert, & Thompson 2005), we assume that the mass loading factor scales inversely with the velocity dispersion.

We identify galaxies using Spline Kernel Interpolative Denmax (SKID), and halos using a spherical overdensity algorithm, as described in Finlator et al. (2006). Our simulation galaxy mass resolution limit is  $M_* > 9.91 \times 10^8 M_\odot$  (i.e. 64 star particles); all predictions regarding galaxies are implicitly for galaxies above this stellar mass.

Our simulations assume a constant metal yield of 0.02, hence metal production directly tracks star formation. Others prefer a value of 1/42 to relate star formation to metal mass production (e.g. Madau et al. 1996). Most of the results presented here will not depend sensitively on this choice, and in fact as long as this value is constant with time, the *fractions* of metals in various phases will be essentially unaffected (modulo small differences due to metal-line cooling). We assume a solar metallicity value of 2% metals by mass.

While we focus on the *vzw* model here, the *mzw* model (the other momentum-driven wind model favored by OD06) produces similar results. We choose the  $32h^{-1}\text{Mpc}$  *vzw* run for this work because it has sufficient resolution to capture early star formation, while still having enough volume to be meaningfully representative at  $z = 0$ . On a practical note, it

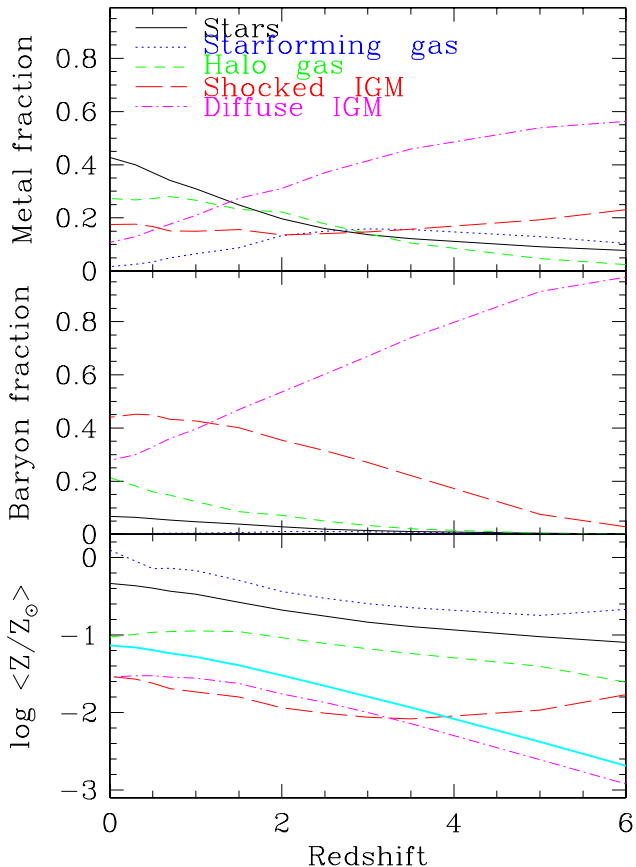


**Figure 1.** *Top:* Metal mass fraction in various baryonic phases as a function of redshift: Stars (black solid), star-forming gas (blue dotted), halo gas (green dashed), shocked IGM ( $T > 10^{4.5} K$ ; red long-dashed), and diffuse IGM (cyan dot-dashed). *Middle:* As above, for total mass fraction of baryons. *Bottom:* As above, for metallicity. The thick cyan line represents the mean mass-weighted metallicity of the universe.

is the only model we have evolved to  $z = 0$ , owing to the significant computational expense involved. We note that cosmic variance could still be significant, and the wind model is as yet not tightly constrained, so the exact values quoted here should be taken as illustrative rather than precise predictions. Using a  $(16h^{-1}\text{Mpc})^3$  volume *vzw* run, we have checked that resolution effects introduce only minor deviations from the numbers quoted herein from  $z = 6 \rightarrow 1.5$ .

Although we are less confident of our predictions at  $z \lesssim 2$  because this particular feedback model has not been critically tested there, we include predictions anyway to illustrate some basic physical trends that are likely to be valid. As we will show later, the comparisons to data at  $z \lesssim 2$  seem to indicate broad agreement.

## 2.2 Metal Mass Fractions

Figure 1 (top panel) shows the evolution of the metal mass fraction in various baryonic phases: Stars, star-forming gas, halo gas, shocked IGM, and diffuse IGM. Middle panel shows the mass fraction in baryons for comparison. Star-forming gas corresponds to gas that is above the density threshold for multi-phase fragmentation in the Springel & Hernquist

(2003a) recipe; this may be thought of as interstellar medium (ISM) gas. Halo gas is defined as gas that is within identified halos but is not star-forming; this includes e.g. hot intracluster gas. Shocked and diffuse IGM gas encompass all gas outside of halos, and are separated by a temperature threshold of 30,000 K (Davé et al. 1999). We choose this threshold as opposed to the canonical warm-hot intergalactic medium (WHIM; Cen & Ostriker 1999; Davé et al. 2001) threshold of  $T > 10^5$  K because in our models, substantial amounts of C IV absorption comes from gas right around  $10^5$  K (OD06), whose temperature is set not by photoionization but by shock heating from outflows and/or gravitational collapse. Hence this gas rightfully belongs in the shocked IGM component.

From  $z \sim 6 \rightarrow 1.5$ , diffuse gas is the largest reservoir of metals; below this, stars take over with halo gas not far behind. It may be surprising that at early times the diffuse phase harbors most metals, given that metals are produced in much denser regions. This arises because early blowout is quite effective in our models, which is required to both enrich the IGM early on and suppress early star formation to match observed high-redshift luminosity functions (Davé, Finlator & Oppenheimer 2006). The diffuse IGM contains virtually all baryons at high redshift as is generically seen in hydrodynamic simulations (e.g. Davé et al. 2001), then drops steadily to around 30% mass fraction by today. The drop in metal fraction tracks the drop in total baryon fraction in this phase.

As galaxies grow and outflows become less effective at polluting the diffuse IGM in our momentum-driven wind scenario, the metal mass fraction that remains locked in stars increases. By  $z \sim 2$ , stars contain 20% of all metals, and by today they hold over 40%. This value is consistent within uncertainties to the value of 52% predicted in the model of Calura & Matteucci (2004). Note that the stellar baryon fraction at  $z = 0$  is 6.8%, which is in agreement with observational estimates (e.g. Bell et al. 2003).

The amount of metals in shocked IGM gas remains fairly stable at 15–20% at all epochs. The mass fraction of baryons in this phase grows almost linearly with redshift up to 45% today. Hence while the shocked IGM contains a significant fraction of all present-day baryons, it does not hold a commensurately large reservoir of metals. Meanwhile, the growth of larger potential wells and reaccretion of IGM metals into halos results in a gradual increase of metal mass in halo gas, up to around one-quarter of all metals today. Halo gas is generally over-enriched relative to its mass fraction.

Star-forming gas shows a mild increase in metal content at early times, but after  $z = 3$  it drops steadily to a very small number at the present epoch. This traces its baryon fraction evolution, which is difficult to see on this plot because it is quite small at all epochs. This shows that galaxies are in general becoming more gas-poor with time, as inflow shuts off because of cosmological acceleration combined with the growth of large potential wells.

In summary, a plausible model of cosmic enrichment that broadly matches key IGM and galaxy metallicity measures predicts that metals are present in a range of baryonic phases from the earliest epochs until the present day. There is no dominant reservoir of metals at any epoch, although diffuse IGM gas holds a significant amount early on (mainly

because virtually all baryons are in this phase), while stars hold the most metals today.

### 2.3 Missing Metals Problem

Observational estimates have now been made for the metal content in various systems at  $z \sim 2.5$ , which as discussed earlier has led to a missing metals problem. Here we present a comparison of our model predictions with various observations that try to account for the missing metals.

At  $z \sim 2 - 3$ , FSB05 and BLP06 estimated that stars in Lyman break galaxies, particularly the BX sample of Shapley et al. (2005), contain about 18% of all metals. BLP06 go on to estimate a contribution of  $\sim 5\%$  from so-called Distant Red Galaxies, though this may have some overlap with the BX sample (Reddy et al. 2005). Our predicted metal fraction in stars is somewhat higher ( $\approx 30\%$ ), which may be explained if our typical stellar mass of LBGs is higher by  $\sim 50\%$  than derived by Shapley et al. (2005). This would easily fall within the substantial uncertainties of spectral energy distribution fitting techniques by which stellar masses are estimated. In general, simulations tend to predict LBGs that have substantial older populations (Finlator et al. 2006), and tend to be more massive than burst-dominated models would predict. Furthermore, there are completeness issues as our simulations include all stars in galaxies down to  $M_* \sim 10^9 M_\odot$ , while typical LBG surveys are substantially incomplete at such masses.

At  $z \sim 0$ , an observational census of metals by Pagel (2002) finds  $\sim 50\%$  in stars today depending on assumptions about the IMF and stellar evolution, which again is in general agreement with our prediction of 43%. If we fix a stellar baryon fraction of 7% as our models predict, then Finoguenov, Burkert & Boehringer (2003) determines  $\Omega_{Z,*} \approx 3 \times 10^{-5}$ , whereas we predict  $2.5 \times 10^{-5}$ , again within uncertainties. In all, while more careful comparisons are warranted, the preliminary indication is that our stellar metal fraction agrees broadly with data, and shows that stars contain a substantial but not dominant fraction of metals in the universe at both high and low redshifts.

Our simulations further predict that about 15% of metals reside in cold star-forming gas in galaxies at  $z = 2.5$ . It has been suggested that Damped Lyman Alpha absorbers (DLAs) may trace this cold dense gas. Yet despite the fact that such systems dominate the H I content of the Universe, they are seen to contain just a few percent of all metals (Prochaska et al. 2006). However, DLAs may just be the tip of the iceberg: Prochaska et al. (2006) and Kulkarni et al. (2006) find sub-DLAs ( $10^{19} < N_{HI} < 10^{20.3} \text{ cm}^{-2}$  systems) with above-solar metallicities, and extrapolate that such systems may represent 15–25% or more of the total metal budget. However, there is a bias towards selecting highly enriched sub-DLAs, so the extrapolations are highly uncertain. We will address sub-DLA metallicities in the next section. Another reservoir of star-forming gas is sub-millimeter galaxies, which are rare but massive and highly enriched; from their gas content and metallicity Bouché, Lehnert & Péroux (2006a) estimated that their ISM may contain  $\sim 5\%$  of the total metals. In general, it seems that the metals in star-forming gas are a relatively small fraction of the total metals, broadly agreeing with our predictions, although if sub-DLAs make as much of a con-

tribution as claimed then perhaps the agreement is not so good.

Combining these constraints, BLP06 determined that approximately 30% of metals are currently observed in galaxies (stars+ISM) at  $z = 2.2$ , which could plausibly increase to 50% with incompleteness corrections. This is quite consistent with our prediction of  $\sim 40\%$  of metals being contained in galaxies with  $M_* \gtrsim 10^9 M_\odot$  at these epochs. In particular, we do not predict, and our models do not require, a substantial amount of metals to be in some hidden form within galaxies.

The remaining 60% of metals are not in the inner regions of galaxies, so have presumably been ejected through galactic outflows (note that the amount actually ejected is much larger, but many metals get reaccreted into halos). Of this, we predict that more than half of that is in the diffuse IGM at  $z \sim 3$ . This is substantially larger than previous estimates. Using two-phase analytic modeling of the IGM, FSB05 estimate that less than 10% of metals are allowed in this diffuse phase (see also Pettini 2004, and references therein). The discrepancy arises because the ionization corrections needed to obtain the metallicity are typically done assuming the metals lie in gas having the density-temperature relation of the Ly $\alpha$  forest. However, our simulations predict that a substantial amount of C IV-absorbing gas is heated to somewhat higher temperatures (see Figure 9 of OD06). Therefore we can hide more C IV in the diffuse phase (defined here as  $T < 10^{4.5}$  K) because our ionization fractions are lower than given by the Ly $\alpha$  equation of state (see Figure 10 of OD06). Note that we still obtain a good fit to the observed  $b$ -parameter and C III/C IV pixel optical depth ratio data, both measures of C IV absorber temperatures, despite this mildly shock-heated absorbing gas.

The remaining 30% of metals in the Universe are divided between shocked IGM gas and halo gas at  $z \sim 2.5$ . FSB05 suggest that up to 90% of all metals may be hidden in hot galactic halo gas; our simulations do not support this idea. The amount in halo gas is difficult to quantify at high redshifts, but an estimate of metals in clusters at  $z \sim 2.5$  by Finoguenov, Burkert & Boehringer (2003) predicts around 10%, rising modestly to 20–25% at  $z \sim 0$ . Our predicted value for halo gas also evolves slowly as well, and the numbers are similar, although a more careful comparison is warranted in order to critically assess how our definition of halo gas relates to gas in clusters or protoclusters.

The fraction of metals in shocked IGM gas, closely related to the missing baryons (Cen & Ostriker 1999) or WHIM gas, is relatively constant. Such gas may be traced by O VI absorbers (Tripp et al. 2006), though because O VI is not the dominant ionization state of this gas (as we will show in §3.2), the uncertainties in the ionization corrections are large (Tripp et al. 2001). Estimates of the metal content of O VI systems by Finoguenov, Burkert & Boehringer (2003) also show little evolution in their metal fraction, though they estimate around one-third of all metals are in this phase as opposed to our predicted values of 15–20%.

So let us return to the original question: Where are the missing metals? According to BLP06 and our models, at least 50% are not in galaxies. The basic answer from our simulations is that they are mostly in gas that has been mildly heated by a combination of gravitational and feedback effects. The enriched diffuse IGM is somewhat warmer

than expected from photoionization alone, the WHIM at these redshifts contains a non-trivial amount, and galactic halos also contain hot gas that has a non-negligible metal content. Hence metals are hidden in hot gas, but that gas is not confined to halos but rather spread among a wide range of overdensities (as we will show in §3.1). Overall, the simulations support a view where metals are rather evenly distributed among the various baryonic phases, which seems to be what observations suggest as well.

## 2.4 Metallicity Evolution

While obtaining a census of total metals is difficult because it requires detecting all metals in a given phase or extrapolating from available data, determining the mean metallicity is somewhat easier as it may have a characteristic value for a given phase of baryons. Hence the observations are somewhat better constrained, and in turn provide interesting constraints on our global enrichment model.

The bottom panel of Figure 1 shows the evolution of the mean mass-weighted metallicity in various phases, along with the global mean shown as the thick cyan line. The global mean metallicity tracks the diffuse IGM metallicity quite well down to  $z \sim 1$ , albeit higher by around 0.2 dex. This is largely because the diffuse phase contains most of the baryons in the Universe until  $z \sim 1$ , where WHIM gas begins to dominate. The global metallicity is around 2-3% solar at  $z = 2.5$  and reaches a present-day value of almost one-tenth solar.

It has been claimed that clusters represent a fair sample of the Universe in terms of galaxy formation processes, because they have a stellar baryon fraction similar to the global value (e.g. Renzini 1998). However our models do not support this idea (and neither do those of Calura & Matteucci 2004). Our predicted hot halo gas metallicity is well above the mean global metallicity at all epochs, and does not evolve similarly. This is primarily because the interplay of outflows with cluster potentials allows larger halos to retain and/or reaccrete more of their metals. In other words, galaxies are significantly affected by their environment not only through structure formation processes, but also through outflow processes.

Stars gain a mean metallicity of  $\gtrsim 1/10$  solar very early on, and in conjunction with a mass-metallicity relation whose slope is established at early times (Davé, Finlator & Oppenheimer 2006), it is not surprising to find massive high-redshift galaxies with solar metallicity (Shapley et al. 2004). The mean stellar metallicity rises steadily from around one-tenth solar at  $z = 6$  to around one-half solar today. This latter value can be compared to observations, though there are difficulties in determining stellar population metallicities owing to degeneracies with age (e.g. Trager et al. 2000). Finoguenov, Burkert & Boehringer (2003) found a mean stellar metallicity of 0.6 solar in galaxy groups, which agrees nicely with our predicted value, assuming that stars in galaxy groups are representative stars everywhere in terms of their metallicity.

Star-forming gas has a mean metallicity that evolves similarly to that of stars, only about a factor of two higher. Observational measures of gas-phase metallicity in galaxies generally rely on emission line tracers that arise in star form-

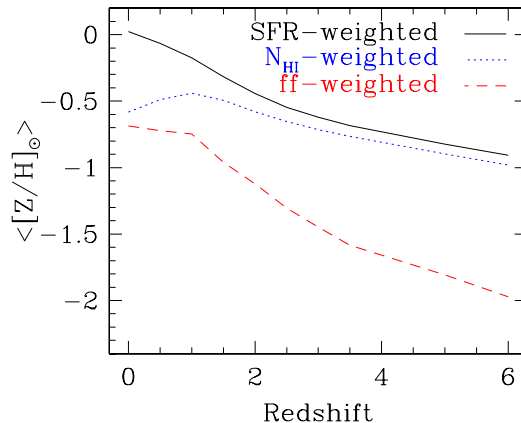


**Figure 2.** Mean gas metallicity weighted by star formation rate (solid), H I column density (dotted blue), and free-free emission (dashed red), as a function of redshift. The first represents the mean metallicity of stars forming at a given redshift, the second corresponds roughly to the mean metallicity in DLAs, and the final one corresponds roughly to the X-ray weighted metallicity of intracluster gas.

ing regions. Hence a more observationally relevant question is: What is the mean metallicity of stars forming today? This can be calculated as the SFR-weighted metallicity.

Figure 2 (solid line) shows the SFR-weighted metallicity as a function of redshift. This weighting is most closely related to the H II region emission line metallicity used to determine, e.g., the mass-metallicity relation in galaxies (e.g. Tremonti et al. 2004). At early epochs, the SFR-weighted metallicity is quite similar to the mean metallicity in stars, but by  $z = 0$  it is roughly twice the stellar one. At the present epoch, our model predicts that stars are forming on average at solar metallicity, although the average star has a metallicity half that.

The metallicity of DLAs provides another constraint on global metallicity evolution. Their H I column density weighted metallicity is seen to evolve slowly from one-tenth solar at  $z \sim 3$  to one-fifth solar at  $z \sim 0.5$ , with some evidence for lower metallicities at  $z \gtrsim 3$  (Péroux et al. 2006). In contrast, models by Pei, Fall & Hauser (1999) and Somerville, Primack & Faber (2001), which match DLA metallicities well at  $z \gtrsim 2$ , predict nearly solar metallicity at  $z \sim 0.5$  for DLAs.

In order to compare our simulations to this data, we determine an H I column density-weighted mean metallicity, shown as the dotted line in Figure 2. This is obtained by calculating the H I ionization fraction assuming a Haardt & Madau (2001) background as described in OD06, and multiplying the H I density by  $\rho^{-1/3}$  to obtain a (scaled) column density for weighting. In broad agreement with data (Péroux et al. 2006), the evolution is fairly mild from  $z \sim 3 \rightarrow 0.5$ , albeit somewhat higher than observed values. In contrast with models mentioned above, our predicted DLA metallicity actually drops from  $z = 1 \rightarrow 0$ , and is distinctly sub-solar by the present epoch.

It is worth noting that our computation of the H I fraction assumes optically thin gas; this is clearly an incorrect assumption in the highly dense regions that may be responsible for DLA absorption. If we make the extreme assumption that every star-forming gas particle is completely neutral

(even though it is likely that at least some portion of the ISM is ionized), then the H I column density-weighted metallicity goes up by 0.2-0.4 dex at  $z \lesssim 2$ . Obviously a more careful analysis is required; we leave this for future work.

The discrepancy between previous predictions and data has spurred investigations of sub-DLAs as being responsible for holding highly enriched H I that may make up the shortfall. Indeed, Prochaska et al. (2006) and Kulkarni et al. (2006) find highly enriched sub-DLAs, and suggest that they may hold substantial amounts of metals, as discussed in §2.3. However, while their metallicities are quite high, this is offset by their lower column densities, so it is unclear whether they raise the global H I metallicity by a large amount. From our models' perspective, there is at most a minor discrepancy to explain: we predict mild evolution and significantly sub-solar metallicities for H I gas even at low redshifts, consistent with observations, though the somewhat higher metallicities overall predicted by our models could certainly accommodate some contribution from highly enriched sub-DLAs.

A tight constraint for the metallicity of hot gas at  $z \approx 0$  is provided by intracluster media, which show a relatively uniform metallicity of around one-third solar. Effectively, this is an X-ray emission weighted metallicity. Figure 2 (dashed line) shows the metallicity of gas with  $T > 10^6$  K weighted by its free-free emission, i.e.  $\rho^2 T^{0.5}$ . The value at  $z = 0$  is around one-fifth solar, which is slightly below that seen in clusters. Note however that our simulation volume does not contain any actual clusters (our largest halo has a virial temperature of around 2 keV), and also free-free emission is a subdominant contribution to the emission at  $T \lesssim 1$  keV where metal lines are prevalent. So the modest disagreement, while intriguing, should be regarded as preliminary. It is still worth noting that we predict little evolution in the emission-weighted metallicity of hot gas to  $z \sim 1$  (in qualitative agreement with data, e.g. Rosati et al. 2004), but at higher redshifts this metallicity drops rapidly.

Shocked IGM metallicity remains relatively constant between one-hundredth and one-fiftieth solar, and at  $z \lesssim 4$  it is very similar to the diffuse phase metallicity. The metallicity at  $z \approx 0$  in this phase may be tested using O VI absorbers at low redshift (e.g. Tripp et al. 2006). Comparisons with simulations suggest that a typical metallicity of one-tenth solar in O VI-absorbing gas at low- $z$  would give rise to a line frequency as observed (Cen et al. 2001; Chen et al. 2003). These studies panted on a metal distribution to hydro simulations post facto. Since our simulations produce a lower mean metallicity than inferred by such studies, it bears testing whether our simulations can reproduce the observed O VI frequency directly from the simulated metal distribution. We are doing this comparison now.

In summary, our models show broad agreement with the observed metallicity evolution as traced by stars, DLAs, and intracluster gas. Clearly more careful comparisons are warranted, but even these comparisons illustrate the power of metal observations in constraining outflow models, and in turn how such models can be used to coherently assemble information from a variety of objects and environments.

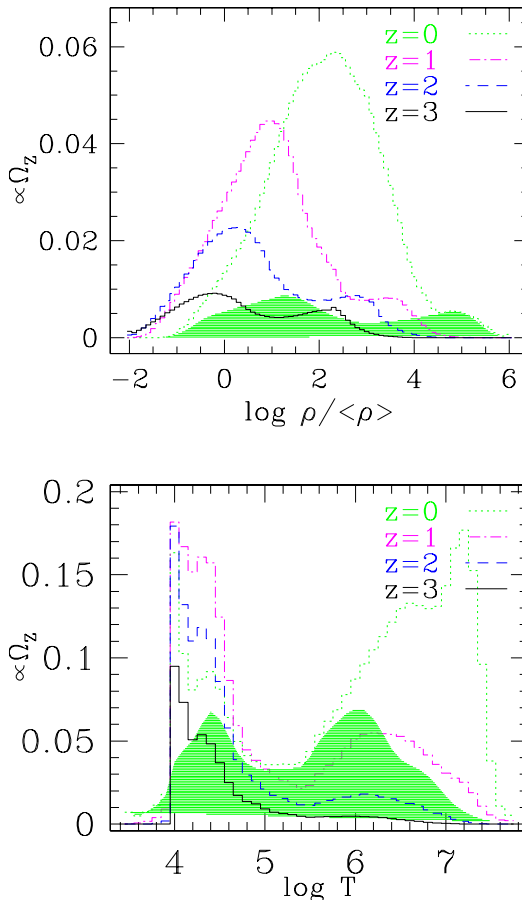


**Figure 3.** Histogram of metal mass in gas as a function of overdensity (top panel), and temperature (bottom) at  $z = 3, 2, 1, 0$ . The area under the histogram is proportional to the total metal mass at that redshift. Shaded regions show the  $z = 0$  histogram for  $T < 10^{4.5}$  K (top) and for  $\rho/\bar{\rho} < 100$  (bottom). The vertical axis values are arbitrary, but are proportional to the total metals mass  $\Omega_Z$ .

### 3 METALS IN PHASE SPACE

#### 3.1 Evolution in Phase Space

The evolution of metals cosmic phase space, i.e. overdensity versus temperature, gives insights into galaxy formation processes. Metals are driven to lower densities through outflows, and to higher densities through gravitational collapse. They are heated by gravitational infall and outflow-induced shocks, and cooled via radiative processes and Hubble expansion. The path of metals in phase space over time is a key prediction of hierarchical galaxy formation models with outflows. Here we describe some general trends of the path of cosmic metals in phase space. We focus here on metals in gaseous form, leaving aside the metals locked into stars.

Figure 3 shows histograms of metal mass as a function of overdensity (top panel) and temperature (bottom), at  $z = 3, 2, 1$  and 0. The overdensity here is taken from the particle densities, hence it is smoothed on the scale of the SPH kernel, which goes from hundreds of kpc in underdense regions to sub-kpc scales in the densest regions; it is the essentially the minimum scale over which density fluctuations can be modeled with this SPH-based code. At all redshifts, metals show a characteristic bimodality in overdensity, with

the diffuse peak holding the majority of metals. At  $z = 3$ , metals are prominent in the diffuse IGM with  $\rho/\bar{\rho} \lesssim 1$ , but are also quite evident in a rather narrow peak at  $\rho/\bar{\rho} \sim 200$  that likely arises because outflows stall as they intercept a dense IGM just outside halos. At  $z = 2$ , the diffuse IGM increasingly dominates the gas metal budget, but the peak has shifted towards higher overdensities. The trend continues at  $z = 1$ , and by  $z = 0$  the peak of metals has shifted to fairly sizeable overdensities, around  $\rho/\bar{\rho} \sim 200$ , and metals are now seen in very dense gas.

The main trend from this is that metals shift to more overdense regions with time, because large halos are able to retain more of their metals. Note that in our simulations this is *not* because outflows escape more easily from small halos. Recall that in our momentum-driven wind model, the outflow velocity scales with the velocity dispersion. Hence all halos, to first order, lose a fixed amount of their ejected material. However, since the mass loading factor scales inversely with the velocity dispersion, smaller halos eject a greater fraction of their star-forming gas, causing them to lose more of their total metal mass. Another factor is that, as star formation shuts off in the more massive halos, the outflows also subside, and the earlier-forming massive halos have more time to reaccrete their metals.

The bottom panel shows the histogram with respect to temperature. Again, a sort of bimodality exists, although it is not obvious until  $z \lesssim 2$ . Very few metals have  $T < 10^4$  K; although the underdense photoionized IGM extends to lower temperatures, the metals are restricted to the denser regions, and have a relatively small filling factor (OD06). Note that the cutoff at high temperatures is an artifact of our small simulation volume, whose largest halo at  $z = 0$  has a virial temperature of  $\approx 2$  keV. While the amount of metals increases at all temperatures, the most notable increase occurs at  $T \gtrsim 10^6$  K. This owes primarily to the growth of large enriched potential wells from surrounding enriched WHIM gas, which is then unable to cool their gas efficiently (Keres et al. 2005). However, this does not imply that cluster metallicities should evolve significantly, because as seen in Figure 1 this evolution is driven mainly by an increase in the baryon fraction in the halo gas phase, while its metallicity remains fairly constant.

The bimodality in both the density and temperature histograms suggests that the peaks may be straightforwardly related. But this is not so. To illustrate this, the shaded region in the top panel of Figure 3 shows the low-temperature ( $T < 10^{4.5}$  K) portion of the  $z = 0$  density histogram, while the shaded region in the bottom panel shows the low-density ( $\rho/\bar{\rho} < 100$ ) portion of the  $z = 0$  temperature histogram. This shows that the high-overdensity peak is comprised primarily of cooler gas, while the major peak at moderate overdensities is mostly shocked gas. In the temperature histogram, the low density gas dominates at  $10^{4.5} \lesssim T \lesssim 10^6$  K (corresponding to WHIM gas), while at  $T \gtrsim 10^6$  K and  $T \lesssim 10^{4.5}$  K one finds higher-density gas.

In summary, gas-phase metals move into hotter, denser regions in the Universe with time, owing to the interplay between early outflows, gravitational reaccretion, and heating by structure formation. At  $z = 2$ , the peak of metals is around the cosmic mean density, in diffuse photoionized gas. By  $z = 0$ , the metals have recollapsed into regions more than 100 times the mean density, with many of the metals

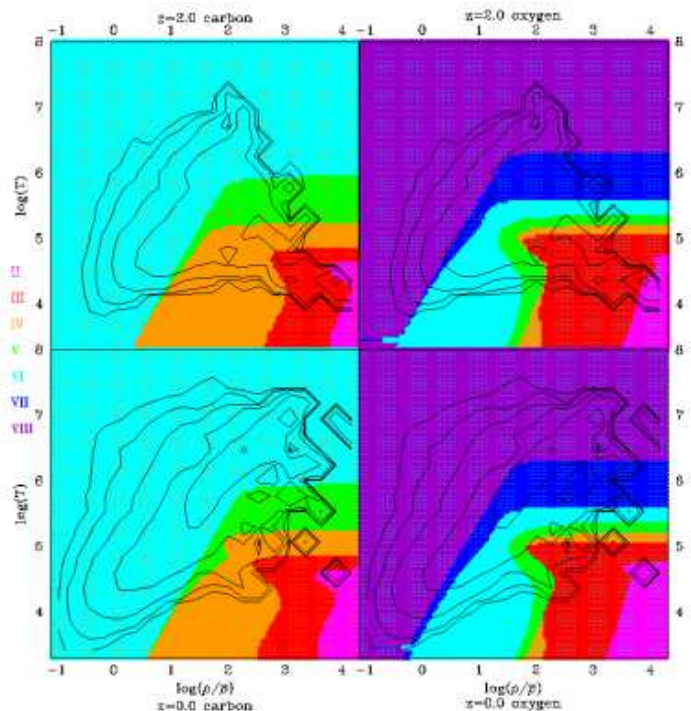


**Figure 4.** Phase space diagrams showing the metal mass (contours) and regions of phase space where the ions shown are the dominant state of carbon (left panels) and oxygen (right), at  $z = 2$  (top panels) and  $z = 0$  (bottom). Exceptions are C IV, O V, and O VI, which are shown when their ionization fraction is above 8% (or else they would not show up at all). Ionization states are colour coded as indicated to the left of the plot.

shock heated to  $T > 10^5$  K. Tracing this evolution directly with observations would provide a stringent test for cosmic enrichment models.

### 3.2 IGM Metal Tracers

How does one observationally catalog metals in various baryonic phases? As discussed in §2.2, metals in ISM gas are probably most straightforward to catalog as they are visible in emission lines, though significant calibration issues remain (e.g. Ellison, Kewley & Mallén-Ornelas 2005). Stars are also fairly straightforward to count, although the age-metallicity degeneracy requires spectroscopy to overcome. Metals in hot gas may be seen in X-rays, which can in principle pick up a significant fraction of metals at  $z = 0$  (Figure 3), but this is limited to low redshift systems having  $T \gtrsim 10^6$  K where the Galactic foregrounds are not overwhelming. The remainder of metals are probably most effectively traced through absorption line spectroscopy against background sources such as quasars, with the most commonly utilized tracers being ultraviolet lines C IV and O VI. In this section we examine how such metal ions can trace the evolution of metals in phase space.

Figure 4 shows a phase space diagram for gas from our simulations, with contours showing metal mass at  $z = 2$  (upper panels) and  $z = 0$  (lower). The evolution of metals in phase space as described in the previous section is evident here, as metals move to hotter, denser gas from  $z = 2 \rightarrow 0$ . At low redshifts some metals do penetrate well into the

voids, affording at least in principle the ability to trace low-density photoionized IGM gas with metal absorption lines, although the ionization levels are quite high.

The coloured bands show regions in phase space where a given ion is the dominant ionization state for that metal. Left panels show carbon, right panels show oxygen, and the colouring goes from singly-ionized (in the lower right area) to highly ionized (in the upper left area). For visibility, C IV, O V, and O VI are always shown when they have ionization fractions above 8%; this is done because those species are never the dominant ionization state, and hence would otherwise not show up on the plot.

The key point to note on this figure is the overlap region between a given ion and the metal mass contours. This corresponds to the range of densities and temperatures that are best traced by that ion. Of course, it is often possible to detect multiple ions for a given system, and the detectability in practice is influenced by other factors such as the oscillator strength and the efficiency of detectors in a given wavelength regime. Hence this plot is only intended to be illustrative of broad trends. Generally, the bands show a characteristic pattern on the plot, with a diagonal rise from low temperatures and densities owing to photoionization, and then a plateau at a particular temperature corresponding to the collisional ionization maximum for that given ion. Note that this plot was computed using CLOUDY (Ferland et al. 1998) with a Haardt & Madau (2001) ionizing background and assuming ionization equilibrium. The photoionized region is somewhat sensitive to our assumed ionizing background, but the collisional ionization plateau is not.

From this plot it is straightforward to see why C IV (1548,1551Å) is a popular absorption feature for tracing IGM metals, being an easily-identifiable doublet at observationally-accessible wavelengths. C IV overlaps the enriched region of phase space from  $\rho/\bar{\rho} \sim 10 - 1000$  with  $T \lesssim 10^5$  K at  $z = 2$ . As OD06 emphasize, C IV becomes a progressively better tracer of bulk IGM metals to higher redshifts. Conversely, to lower redshifts it shifts to higher overdensities and becomes a poorer tracer of IGM metals. C VI (33.7Å) is more optimal for tracing photoionized IGM metals and C V (40.3Å) nicely tracks the bulk of metals (and gas) in the WHIM regime, but both lie in the observationally challenging soft X-ray regime. At  $z = 2$ , C III (977Å) tracks the metals in cool gas around galaxies, but by  $z = 0$  it is predicted to be uncommon because there are few metals left in such dense regions, as it has mostly been consumed in star formation or shock-heated to higher temperatures. C II (1335Å) traces gas in the inner regions of galactic halos, which likely involves multi-phase gas clumps for which it becomes difficult to interpret line ratios. Hence until significant advances are made in soft X-ray spectrographs, carbon is in practice only effective for tracing IGM metals at  $z \gtrsim 2$ .

Oxygen has the advantage of being a highly abundant element, and if starburst ejectae from Type II supernovae are primarily responsible for enriching the IGM, may be alpha-enhanced relative to carbon. Furthermore, a wide range of oxygen lines are observationally accessible and fairly strong. The most common line used to see IGM metals is O VI (1032,1037Å), which traces a wide range of environments from photoionized gas around the cosmic mean up to WHIM gas at overdensities around a thousand. Indeed, disentangling the photoionized O VI absorbers versus the

collisionally ionized ones is challenging (Tripp et al. 2001, 2006). At  $z \gtrsim 2.5$  this line starts to become overwhelmed by the thickening Ly $\alpha$  forest (Simcoe, Sargent & Rauch 2004). O VII (21.6Å) and O VIII (19Å) trace the majority of WHIM metals (e.g. Chen et al. 2003), as well as covering the bulk of the photoionized metals at lower redshifts. However, being that these are X-ray lines, the photoionized regions have too low densities to provide detectable absorption at current sensitivities, and the warm-hot systems are only seen with great effort (Nicastro et al. 2005, though this detection is controversial; see (Kaastra et al. 2006) and (Rasmussen et al. 2006)). Lower ionization lines like O V (630Å) and O IV (787Å) are interesting; although they do not dominate over a wide swath of phase space, it may be possible to detect them with UV instruments in conjunction with O VI at moderate redshifts ( $z \gtrsim 1$ ), enabling detailed studies of the physical conditions and metallicity of  $T \sim 10^5$  K absorbers. O III (702Å) traces denser, colder gas which at  $z \gtrsim 2$  contains substantial amounts of metals, and O II, like C II, is limited to the regions immediately around star-forming gas.

In the future it may be possible to detect IGM metal lines in emission, though this will require a new UV-capable instrument such as the proposed Baryonic Structure Probe (Sembach et al. 2005). The most natural ions to target from a practical standpoint are as usual O VI and C IV, because UV detectors are efficient down to  $\sim 1000\text{Å}$ . However, it would be highly desirable to have detector capabilities extending down to  $\sim 700\text{Å}$ , so that a suite of O III-O VI can be seen in relatively nearby large-scale structure where the emission is not hopelessly dimmed by surface brightness effects. There is also development underway for X-ray imaging with the Diffuse Intergalactic Oxygen Surveyor (Ohashi et al. 2006). Imaging offers the opportunity in principle to directly trace the filamentary topology of WHIM gas, providing another interesting test of models.

In summary, performing a full inventory of metals in intergalactic gas will require next-generation UV and X-ray spectrographs capable of detecting species that sample a wide range of ionization conditions. To this end, oxygen seems more promising than carbon, as O III to O VI are all accessible in the UV, and O VII and O VIII are relatively strong X-ray lines, with oxygen being a highly abundant element. With statistical information on at least several of these lines for a large number of systems, it will become possible to observationally characterize the metal distribution (along with the density and temperature distribution) of IGM gas, and directly test model predictions. For the time being, we are mostly limited to studying single ions in a small number of systems, and inferring the total metal mass from indirectly determined ionization conditions or by comparing with models such as the ones presented here.

## 4 CONCLUSIONS

Using cosmological hydrodynamic simulations of galaxy formation including galactic outflows, we have studied the distribution and evolution of metals in various baryonic phases in the Universe. Our main conclusions are summarized as follows:

- Metals are present in substantial amounts in a wide

range of environments from the earlier epochs studied ( $z \sim 6$ ) until the present. Diffuse IGM gas dominates the metal budget early on, while stars and shocked gas hold most of the metals today.

- The missing metals (outside of galaxies) at  $z \sim 2.5$  are mainly in intergalactic gas that is mildly hotter than pure photoionization temperatures, having  $10^4 \lesssim T \lesssim 10^5$  K. However, this gas is not confined to halos, but is spread across a wide range of overdensities, with a peak around the cosmic mean density.

- Comparisons of our simulation to observations broadly show agreement in the amount of metals in various baryonic phases, and show that metals are spread relatively evenly across all phases.

- The global mean metallicity tracks about 50% higher than the diffuse IGM metallicity from  $z = 6 \rightarrow 1$ , after which it continues increasing to about one-tenth solar at the present epoch. Hot halo gas, which is predicted to have a luminosity-weighted metallicity of around one-fifth solar today, does not track the global metallicity, suggesting that clusters are unlikely to be representative samples of the universe at large. This conclusion comes with a significant caveat, however, as our simulation volume is too small to produce actual clusters, so improved simulations are needed to confirm this.

- Stars and star-forming gas quickly obtain a mean metallicity of  $\gtrsim 0.1Z_{\odot}$  solar at  $z \sim 6$ , indicating early enrichment in galaxies. Today stars have a mean metallicity of one-half solar, while stars just forming now have typically solar metallicity.

- Our models predict a global HI column density-weighted metallicity that increases slowly with redshift from  $z = 6 \rightarrow 1$ , and then actually decreases to  $z = 0$ , never exceeding around one-third solar. This is broadly consistent with observations of DLA metallicities, and does not require a substantial contribution from sub-DLAs.

- Metals generally move from lower temperature and more diffuse regions at early epochs towards hotter, more overdense regions at low redshifts. This occurs because early blowout is very efficient at enriching diffuse gas, while at lower redshift outflows subside and large potential wells reaccrete gas.

- Oxygen, particularly O III–O VII, provides the most effective tracer of metals across a wide range of cosmic phase space at  $z \lesssim 2$ , but a full metal accounting in the IGM will probably require next-generation instruments.

Obtaining a complete census of metals in the Universe will require a concerted effort in studying a variety of systems and environments at various epochs. Still, there is a realistic possibility of providing a full census of metals in the Universe in the foreseeable future. This is certainly a formidable challenge for upcoming facilities, but the payoff is large. By comparing such observations with cosmological simulations of outflows that track the interplay between various baryonic phases in mass, metals, and energy, it will be possible to stringently constrain models of galaxy formation and feedback. This will dramatically advance our understanding of how galaxies and intergalactic gas interact in the cycle of accretion and feedback, and provide for the first time a complete view of how baryons evolve in cosmic phase space from the dark ages until the present.

## ACKNOWLEDGEMENTS

We thank MPIA and H.-W. Rix for their hospitality during the writing of this paper. The simulation used here was run on *grendel*, our department's Beowulf system at the University of Arizona. Support for this work, part of the Spitzer Space Telescope Theoretical Research Program, was provided by NASA through a contract issued by the Jet Propulsion Laboratory, California Institute of Technology under a contract with NASA. Support for this work was also provided by NASA through grant number HST-AR-10647.01 from the SPACE TELESCOPE SCIENCE INSTITUTE, which is operated by AURA, Inc. under NASA contract NAS5-26555.

## REFERENCES

- Barth, A. J., Martini, P. Nelson, C. H., Ho, L. C. 2003, *ApJ*, 594, L95
- Becker, G. D., Sargent, W. L. W., Rauch, M., Simcoe, R. A. 2006, *ApJ*, 640, 69
- Bell, E. F., McIntosh, D. H., Katz, N., Weinberg, M. D. 2003, *ApJ*, 585, L117
- Bouché, N., Lehnert, M. D., Péroux, C. 2006, *MNRAS*, 364, 319
- Bouché, N., Lehnert, M. D., Péroux, C. 2006, *MNRAS*, 367, L16 [BLP06]
- Calura, F. & Matteucci, F. 2004, *MNRAS*, 351, 384
- Calura, F. & Matteucci, F. 2006, *MNRAS*, 369, 465
- Cen, R. & Ostriker, J. P. 1999, *ApJ*, 514, 1
- Cen, R. & Ostriker, J. P. 1999, *ApJ*, 519, L109
- Cen, R., Tripp, T. M., Ostriker, J. P., Jenkins, E. B. 2001, *ApJ*, 559, L5
- Chen, X., Weinberg, D. H., Katz, N., & Davé, R. 2003, *ApJ*, 594, 42
- Davé, R., Hernquist, L., Katz, N., & Weinberg, D. H. 1999, *ApJ*, 511, 521
- Davé, R., Cen, R., Ostriker, J. P., Bryan, G. L., Hernquist, L., Katz, N., Weinberg, D. H., Norman, M. L., & O'Shea, B. 2001, *ApJ*, 552, 473
- Davé, R., Finlator, K., & Oppenheimer, B. D. 2006, *MNRAS*, in press, astro-ph/0511532
- Eisenstein, D. J. & Hu, W. 1999, *ApJ*, 511, 5
- Ellison, S. L., Kewley, L. J., Mallén-Ornelas, G. 2005, *MNRAS*, 357, 354
- Erb, D. K., Shapley, A. E., Pettini, M., Steidel, C. C., Reddy, N. A., & Adelberger, K. L. 2006, *ApJ*, accepted, astro-ph/0602473
- Ferland, G., Korista, K. T., Verner, D. A., Ferguson, J. W., Kingdon, J. B., Verner, E. M. 1998, *PASP*, 110, 761
- Ferrara, A., Scannapieco, E., Bergeron, J. 2005, *ApJ*, 634, L37 [FSB05]
- Finlator, K., Davé, R., Papovich, C., & Hernquist, L. 2006, *ApJ*, 639, 672
- Finoguenov, A., Burkert, A., Boehringer, H. 2003, *ApJ*, 594, 136
- Haardt, F. & Madau, P. 2001, in *proc. XXXVIth Rencontres de Moriond*, eds. D.M. Neumann & J.T.T. Van.
- Kaasra, J. S., Werner, N., den Herder, J. W. A., Paerels, F. B. S., de Plaa, J., Rasmussen, A. P., de Vries, C. P. 2006, *ApJ*, submitted, astro-ph/0604519

- Katz, N., Weinberg, D. H., & Hernquist, L. 1996, *ApJS*, 105, 19
- Keres, D., Katz, N., Weinberg, D. H., & Davé, R. 2005, *MNRAS*, in press
- Kulkarni, V. P., Khare, P., Péroux, C., York, D. G., Lauroeach, J. T., Meiring, J. D. 2006, *ApJ*, submitted, astro-ph/0608126
- Madau, P., Ferguson, H. C., Dickinson, M. E., Giavalisco, M., Steidel, C. C., Fruchter, A. 1996, *MNRAS*, 283, 1388
- Martin, C. L. 2005, *ApJ*, 621, 227
- Murray, N., Quatert, E., & Thompson, T. A. 2005, *ApJ*, 618, 569
- Nicastro, F., Mathur, S., Elvis, M., Drake, J., Fiore, F., Fang, T., Fruscione, A., Krongold, Y., Marshall, H., Williams, R. 2005, *ApJ*, 629, 700
- Ohashi, T. et al. 2006, in proc. SPIE "Astronomical Telescopes and Instrumentation", astro-ph/0607127
- Oppenheimer, B. D. & Davé, R. 2006, *MNRAS*, submitted, astro-ph/0605651 [OD06]
- Pagel, B. E. J. 2002, in "Chemical Enrichment of Intracluster and Intergalactic Medium", ASP conf. proc. v.253, eds. R. Fusco-Femiano and F. Matteucci, p.489
- Pei, Y. C., Fall, S. M., Hauser, M. G. 1999, *ApJ*, 522, 604
- C. Péroux, J. D. Meiring, V. P. Kulkarni, R. Ferlet, P. Khare, J. T. Lauroesch, G. Vladilo, D. G. York 2006, *MNRAS*, accepted, astro-ph/0607561
- Pettini, M. 1999, in proc. ESO Workshop: 'Chemical Evolution from Zero to High Redshift', eds. J. Walsh & M. Rosa, astro-ph/9902173
- Pettini, M. 2004, in proc. "Cosmochemistry. The melting pot of the elements", eds. C. Esteban, R. J. Garcí López, A. Herrero, F. Sánchez, Cambridge, UK: Cambridge University Press, p.257
- Prochaska, J. X., O'Meara, J. M., Herbert-Fort, S., Burles, S., Prochter, G. E., Bernstein, R. A. 2006, *ApJ*, submitted, astro-ph/0606573
- Rasmussen, A. P., Kahn, S. M., Paerels, F., den Herder, J. W., Kaastra, J., de Vries, C. 2006, *ApJ*, submitted, astro-ph/0604515
- Reddy, N. A., Erb, D. K., Steidel, C. C., Shapley, A. E., Adelberger, K. L., Pettini, M. 2005, *ApJ*, 633, 748
- Renzini, A. 1998, in "The Birth of Galaxies", eds. Guiderdoni, B. et al., astro-ph/9810304
- Rosati, P. et al. 2004, *AJ*, 127, 230
- Rupke, D. S., Veilleux, S., & Sanders, D. B. 2005, *ApJS*, 160, 115
- Ryan-Weber, E. V., Pettini, M., & Madau, P. 2006, *MNRAS*, accepted, astro-ph/0607029
- Savaglio, S. et al. 2005, *ApJ*, 635, 260
- Sembach, K. R. et al. 2005, *BAAS*, 23.09, v. 37, p. 1197
- Shapley, A. E., Erb, D. K., Pettini, M., Steidel, C. C., Adelberger, K. L. 2004, *ApJ*, 612, 108
- Shapley, A. E., Steidel, C. C., Erb, D. K., Reddy, N. A., Adelberger, K. L., Pettini, M., Barmby, P., Huang, J. 2005, *ApJ*, 626, 698
- Simcoe, R. A., Sargent, W. L. W., Rauch, M. 2004, *ApJ*, 606, 92
- Simcoe, R. A. 2006, *ApJ*, submitted, astro-ph/0605710
- Somerville, R. S., Primack, J. R., Faber, S. M. 2001, *MNRAS*, 320, 504
- D. N. Spergel *et al.*, *ApJS*, 148, 175
- Springel, V. & Hernquist, L. 2002, *MNRAS*, 333, 649
- Springel, V. & Hernquist, L. 2003, *MNRAS*, 339, 289
- Sutherland, R. S. & Dopita, M. A. 1993, *ApJS*, 88, 253
- Thacker, R. J., Scannapieco, E., Davis, M. 2002, *ApJ*, 581, 836
- Trager, S. C., Faber, S. M., Worthey, Guy, González, J. Jesús 2000, *AJ*, 119, 1645
- Tremonti, C. A., Heckman, T. M., Kauffmann, G., et al. 2004, *ApJ*, 613, 898
- Tripp, T. M., Giroux, M. L., Stocke, J. T., Tumlinson, J., Oegerle, W. R. 2001, *ApJ*, 563, 724
- Tripp, T. M., Bowen, D. V., Sembach, K. R., Jenkins, E. B., Savage, B. D., Richter, P. 2006, in "Astrophysics in the Far Ultraviolet: Five Years of Discovery with FUSE", eds. G. Sonneborn, H. Moos, and B-G Andersson, ASPC v.348, p.341